KINEMATIC DOWNSIZING AT $z\sim 2$

Raymond C. Simons[1], Susan A. Kassin[2], Jonathan R. Trump[3†], Benjamin J. Weiner[4], Timothy M. Heckman[1], Guillermo Barro[5], David C. Koo[6], Yicheng Guo[6], Camilla Pacifici[7^], Anton Koekemoer[2], and Andrew W. Stephens[8]

[1]Johns Hopkins University, Baltimore, MD, 21218, USA; rsimons@jhu.edu
[2]Space Telescope Science Institute, 3700 San Martin Drive, Baltimore, MD, 21218, USA
[3]Department of Astronomy and Astrophysics and Institute for Gravitation and the Cosmos, 525 Davey Lab, The Pennsylvania State University, University Park, PA 16802, USA
[4]Steward Observatory, 933 N. Cherry St, University of Arizona, Tucson, AZ 85721, USA
[5]Department of Astronomy, University of California Berkeley, 501 Campbell Hall, Berkeley, CA 94720, USA
[6]UCO/Lick Observatory, Department of Astronomy and Astrophysics, University of California, Santa Cruz, CA 95064, USA
[7]Astrophysics Science Division, Goddard Space Flight Center, Code 665, Greenbelt, MD 20771, USA
[8]Gemini Observatory, Northern Operations Center, 670 N A'ohoku Place, Hilo, HI 96720
[†]Hubble Fellow
[^]NASA Postdoctoral Program Fellow

Draft version June 2, 2016

ABSTRACT

We present results from a survey of the internal kinematics of 49 star-forming galaxies at $z\sim 2$ in the CANDELS fields with the Keck/MOSFIRE spectrograph (SIGMA, Survey in the near-Infrared of Galaxies with Multiple position Angles). Kinematics (rotation velocity V_{rot} and integrated gas velocity dispersion σ_g) are measured from nebular emission lines which trace the hot ionized gas surrounding star-forming regions. We find that by $z\sim 2$, massive star-forming galaxies ($\log M_*/M_\odot \gtrsim 10.2$) have assembled primitive disks: their kinematics are dominated by rotation, they are consistent with a marginally stable disk model, and they form a Tully-Fisher relation. These massive galaxies have values of V_{rot}/σ_g which are factors of 2–5 lower than local well-ordered galaxies at similar masses. Such results are consistent with findings by other studies. We find that low mass galaxies ($\log M_*/M_\odot \lesssim 10.2$) at this epoch are still in the early stages of disk assembly: their kinematics are often supported by gas velocity dispersion and they fall from the Tully-Fisher relation to significantly low values of V_{rot}. This "kinematic downsizing" implies that the process(es) responsible for disrupting disks at $z\sim 2$ have a stronger effect and/or are more active in low mass systems. In conclusion, we find that the period of rapid stellar mass growth at $z\sim 2$ is coincident with the nascent assembly of low mass disks and the assembly and settling of high mass disks.

Subject headings: galaxies: evolution - galaxies: formation -galaxies: fundamental parameters - galaxies: kinematics and dynamics

1. INTRODUCTION

The cosmic star-formation rate peaks between $z = 1.5$ and $z = 2.5$ (Madau & Dickinson 2014) and marks a critical period for galaxy assembly. In the classic model of galaxy formation, collisional baryons cool and dissipate into the center of dark matter halos while conserving primordial angular momentum, leading to the formation of a thin rotating disk galaxy (Fall & Efstathiou 1980; Mo, Mao & White 1998). Although this gas is expected to

Agertz & Kravtsov 2015).

These processes are prominent at $z\sim 2$, coincident with the assembly of stellar mass in galaxies and may play a stronger role in the shallow potential wells that host low mass galaxies. In general, the formation and development of a galaxy depends strongly on its mass. Massive galaxies tend to assemble their stellar mass first ("downsizing", e.g., Cowie et al. 1996; Brinchmann & Ellis 2000; Juneau et al. 2005) and develop disks earlier (e.g., Kassin et al. 2012; van der Wel et al. 2014b).

Формирование дисков

- Z=1.5- 2 – эпоха max SF. Диски “thick and gas rich”.
  - ЧТО ПРОИСХОДИТ С ДИСКАМИ?
- Продолжающаяся аккреция
- Merging
- Крупномасштабные неустойчивости
- Stellar (and AGN) feedback
- Маломассивные галактики формируют диски медленнее, и на Z~1.5 имеют вытянутую структуру (wan der Wel+2014, Tomassetti +, 2016).
- Как и когда диски переходят к спокойному равновесному состоянию?

Наблюдения

- Keck multi-object near-IR spectrograph +HST imaging
- Цель – исследование кинематики дисков на 1.3<z<1.8 и 2.0<Z<2.5 в трех полях (GOODS-S, GOODS-N and UDS of the HST/WFC3 survey). This survey is named SIGMA.
- Всего- 49 галактик.
- Измерялись: rest I; rest V; PA; b/a; M_*(broadband SED model); SFR (from IR Hershel +UV Spitzer); Vrot, \sigma up to D_50

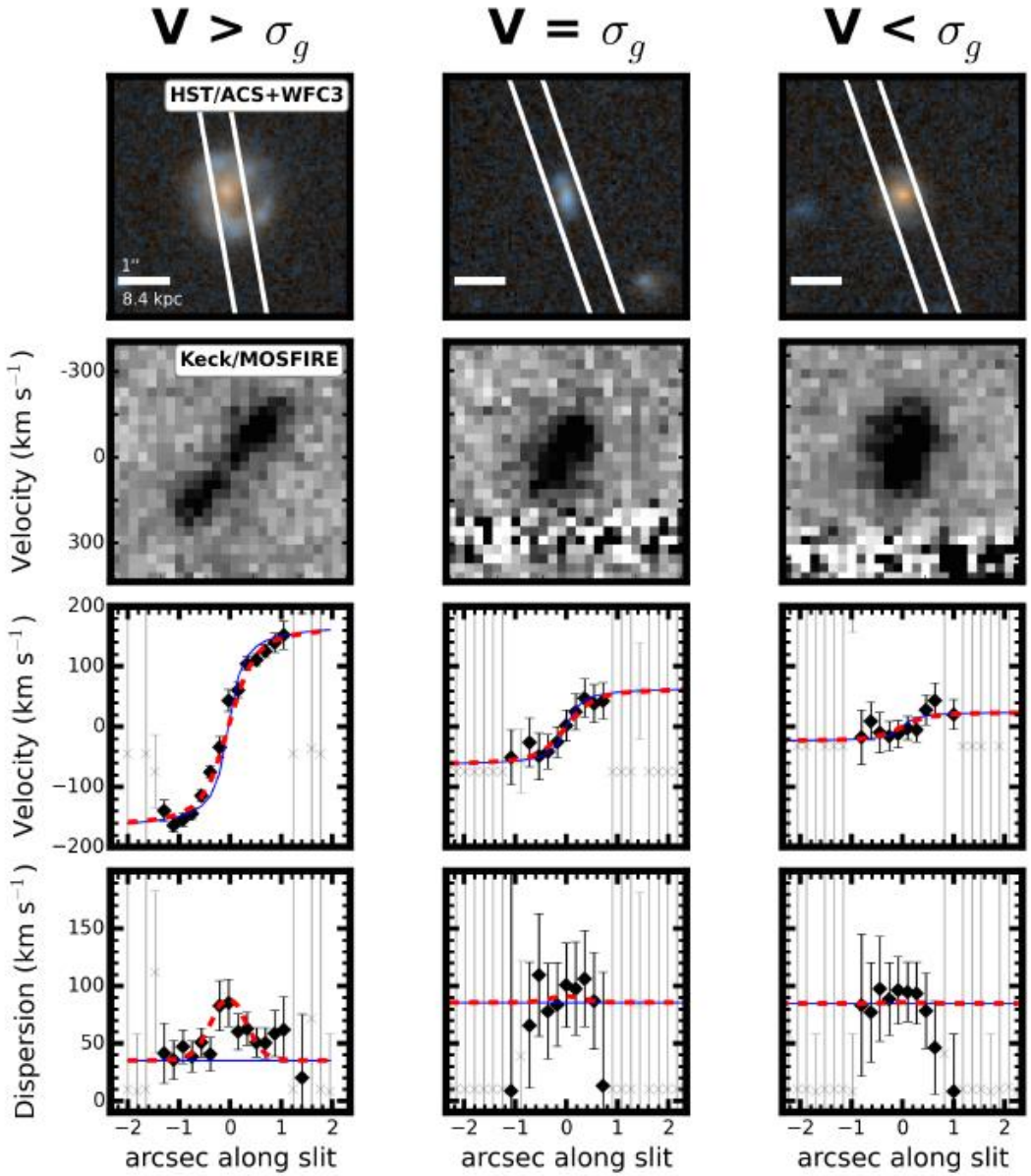

FIG. 3.— Example single slit observations are presented for three SIGMA galaxies (ID: 16600, 16209, 14602). These galaxies span the kinematic types in our sample: a rotation dominated galaxy (left column), a galaxy with equal contributions of rotation and dispersion (middle column), and a dispersion dominated galaxy (right column). In the top two rows we show the I+H-band HST/ACS-WFC3 color images with the MOSFIRE slit placement and the 2-D spectra centered around the Hα line. Strong NIR atmospheric lines are present in the middle and right columns. In the bottom two rows we show the kinematic model fits to the emission lines. The black filled diamonds represent the gaussian fits to the velocity and velocity dispersion in each row of each spectrum. The grey points are poor fits and are discarded. The best-fit models are shown as red solid lines and the intrinsic (pre-seeing blurred) models are shown as blue dashed lines. All of the rows are spatially aligned and each panel is 4.5″ on a side. Kinematic fits for all of the SIGMA galaxies are available in the Appendix.

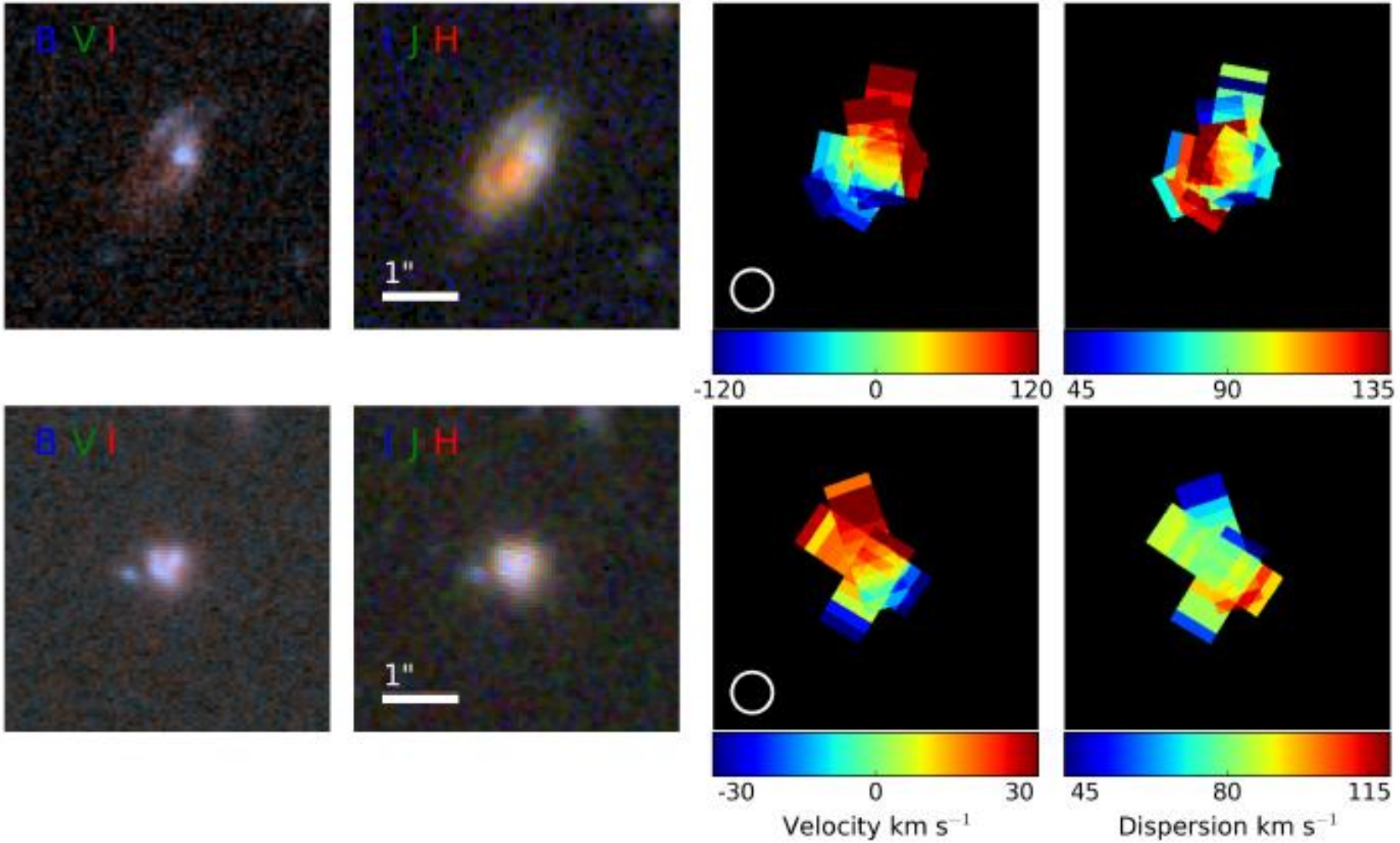

FIG. 4.— Hubble images and reconstructions of 2D kinematic fields from multi-slit observations are shown for two SIGMA galaxies (I 26736, 21162). In the first two columns we show the the HST/ACS optical (rest UV) and the HST/WFC3 near-IR (rest optical) co images, respectively. In the third and fourth columns, we show the co-added velocity ($V \times \sin i$) and velocity dispersion maps, respective The top row shows a regularly rotating disk galaxy: the velocity field has a smooth rotation gradient with a centrally peaked veloc dispersion, both kinematic signatures of a rotating disk. The bottom row shows a dispersion dominated galaxy with complex morpholo and kinematics: it exhibits velocity gradients in orthogonal slits. Each slit pixel is $0.18''$ and the slits are $0.7''$ wide. The typical seeing the H-band is $0.6''$, as shown by the white circles on the velocity maps.

- $\log S_{0.5} = (V^2_{rot}/2 + \sigma_g{}^2)^{1/2}$

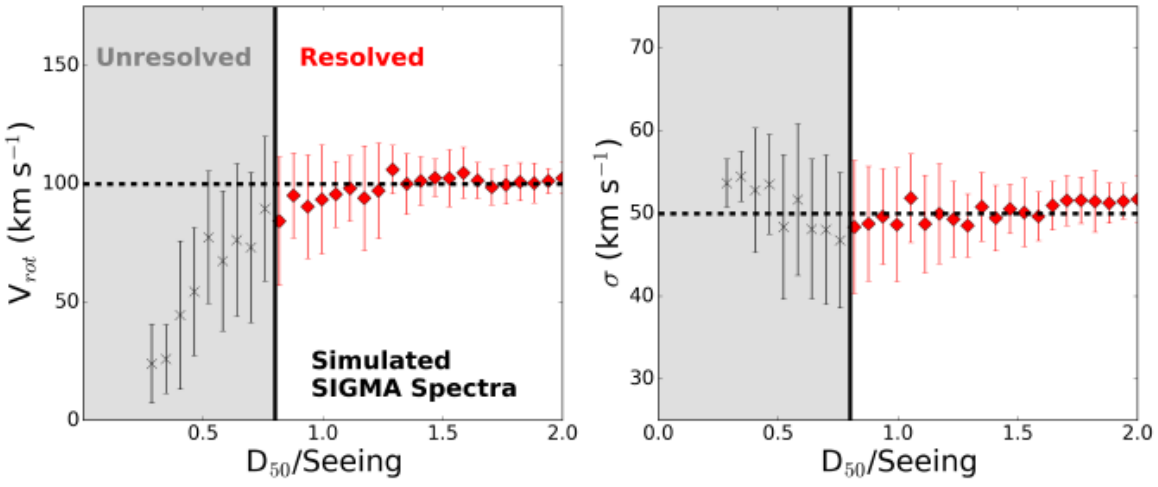

FIG. 8.— Our models demonstrate that galaxy kinematics in SIGMA can be measured down to a size of $D_{50} = 0.8 \times Seeing_{FWHM}$, where D_{50} is the intrinsic half-light diameter and $Seeing_{FWHM}$ is the full width at half maximum of the seeing during the observations. These plots show mock observations of a model galaxy at varying intrinsic sizes, the points show the mean and rms scatter from 100 realizations at each size interval. The model is a rotation dominated galaxy with $V_{rot} = 100$ km s^{-1} and $\sigma_g = 50$ km s^{-1}, marked by the dashed line, and the emission line profile is a Sersic with an index of $n = 2$. The correct values of V_{rot} (left panel) and σ_g (right panel) are recovered (red circles) for mock observations with intrinsic sizes $D_{50} > 0.8 \times Seeing_{FWHM}$. We find a systematic drop in V_{rot} and a slight increase in σ_g for models that have sizes smaller than this value and are unresolved (black x's).

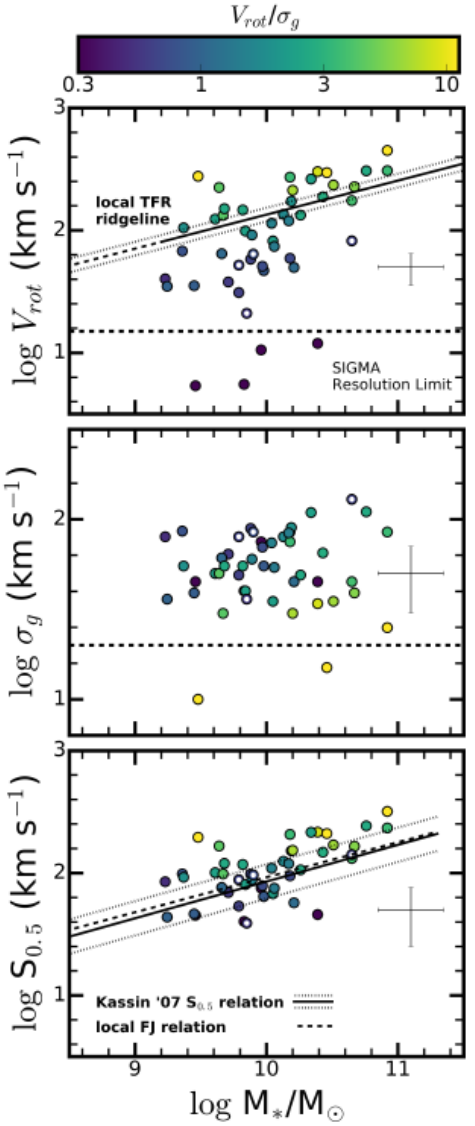

3. 5.— Top: The Tully-Fisher (TF) relation for SIGMA shows ificant scatter to low V_{rot} from the local TF ridge line, defined Reyes et al. 2011. The largest scatter is found at low stellar s (log $M_*/M_\odot \lesssim 10.2$). Middle: The relation between inte- ed gas velocity dispersion (σ_g) and M_* is shown. The slowly ting galaxies that fall from the TF relation have elevated veloc- lispersions. Bottom: The $S_{0.5}$ TF relation is shown along with fit and scatter from the $z \sim 0.2$ DEEP2 sample (Kassin et al. 7) and the local Faber-Jackson relation, defined by Gallazzi et 006. The handful of galaxies in which the largest velocity gra- t was measured in an off-axis slit are not inclination corrected are shown as open circles. The resolution limits for measur- rotation and dispersion in SIGMA is given by the horizontal ed lines in the top and middle plots.

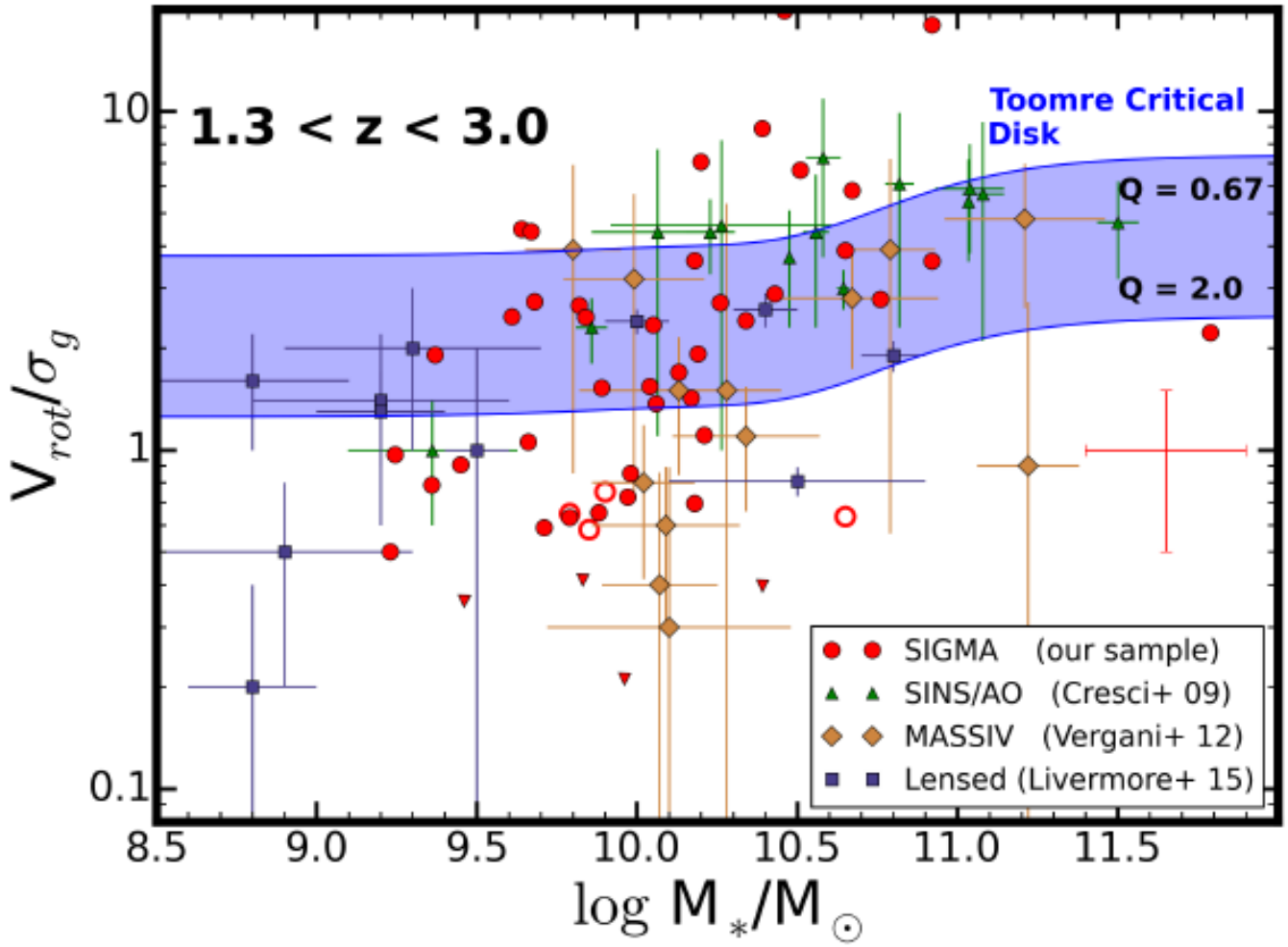

FIG. 7.— Kinematic order (V_{rot}/σ_g) versus stellar mass for galaxies in SIGMA and from the literature. A model for a marginally sta disk galaxy at $z \sim 2$ is shown as a blue shaded swath. While high mass galaxies fall within this swath, a large fraction of the low m galaxies fall below it. High mass galaxies at $z \sim 2$ are consistent with the model, implying that they have already formed primitive di In contrast, a large fraction of the low mass galaxies are dispersion dominated ($V_{rot}/\sigma_g < 1$) and are still in the process of assembl their disks. We note that the high mass disks are unlike the majority of local disk galaxies at a similar stellar mass, which typically h values of V_{rot}/σ_g of around 10-15.

Основные выводы

- Массивные галактики (log M_*>10.2) на z=2

обладают дисками с упорядоченным вращением , соответствующим локальной TF –зависимости, но с большой дисперсией скоростей газа.

- Маломассивные галактики – на ранней стадии формирования

диска, у них дисп.скоростей газа порядка или выше скорости вращения.

- Упорядоченное вращение (высокое значение Vrot/σgas)

коррелирует в большей степени с массой звезд, чем с SFR или массой газа (downsizing). Значит, высокая σgas поддерживается не SF, а другими (гравитационными?) механизмами.

Low mass galaxies tend to be more in the early process of assembling their disks. The peak of cosmic star-formation is coincident with the epoch of disk assembly for low mass galaxies and the settling of primitive disks in high mass galaxies.

A Tale of Two Tails: Exploring Stellar Populations in the Tidal Tails of NGC 3256

Michael Rodruck,[1⋆] Iraklis Konstantopoulos,[2] Karen Knierman,[3,4] Konstantin Fedotov,[5,6] Brendan Mullan,[7,8] Sarah Gallagher,[5] Patrick Durrell,[9] Robin Ciardullo,[1,10] Caryl Gronwall,[1,10] and Jane Charlton[1]

[1] *Department of Astronomy and Astrophysics, The Pennsylvania State University, University Park, PA 16802, USA*
[2] *Australian Astronomical Observatory, North Ryde, NSW 2133, Australia*
[3] *School of Earth & Space Exploration, Arizona State University, 550 E. Tyler Mall, Room PSF-686 (P.O. Box 871404), Tempe, AZ 85287-1404, USA*
[4] *NSF Astronomy and Astrophysics Postdoctoral Fellow*
[5] *University of Western Ontario, London, ON N6A 3K7, Canada*
[6] *Herzberg Institute of Astrophysics, National Research Council of Canada, Victoria, BC V9E 2E7, Canada*
[7] *Point Park University Natural Sciences and Engineering Department 201 Wood St Pittsburgh PA 15222, USA*

ABSTRACT

We have developed an observing program using deep, multiband imaging to probe the chaotic regions of tidal tails in search of an underlying stellar population, using NGC 3256's 400 Myr twin tidal tails as a case study. These tails have different colours of $u-g=1.05\pm0.07$ and $r-i=0.13\pm0.07$ for NGC 3256W, and $u-g=1.26\pm0.07$ and $r-i=0.26\pm0.07$ for NGC 3256E, indicating different stellar populations. These colours correspond to simple stellar population ages of 288^{+11}_{-54} Myr and 841^{+125}_{-157} Myr for NGC 3256W and NGC 3256E, respectively, suggesting NGC 3256W's diffuse light is dominated by stars formed after the interaction, while light in NGC 3256E is primarily from stars that originated in the host galaxy. Using a mixed stellar population model, we break our diffuse light into two populations: one at 10 Gyr, representing stars pulled from the host galaxies, and a younger component, whose age is determined by fitting the model to the data. We find similar ages for the young populations of both tails, (195^{-13}_{+0} and 170^{-70}_{+44} Myr for NGC 3256W and NGC 3256E, respectively), but a larger percentage of mass in the 10 Gyr population for NGC 3256E (98^{+1}_{-3}% vs 90^{+5}_{-6}%). Additionally, we detect 31 star cluster candidates in NGC 3256W and 19 in NGC 2356E, with median ages of 141 Myr and 91 Myr, respectively. NGC 3256E contains several young (< 10 Myr), low mass objects with strong nebular emission, indicating a small, recent burst of star formation.

Q. Из каких звезд состоят tidal tales (TT)? Много ли старых звезд? Где формируются

Программа ugriz –фотометрии диффузного света TT системы NGC3256

Расстояние

T_collision~400 Myr

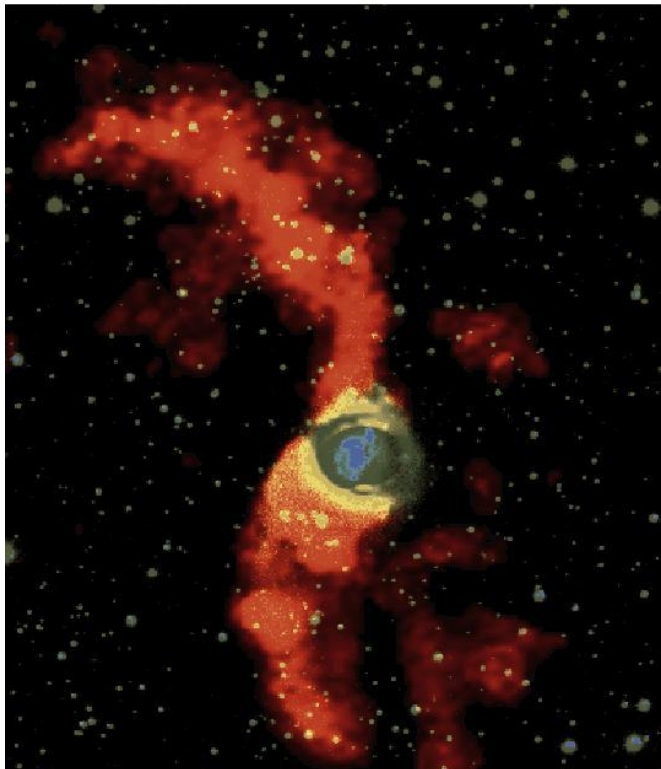

- Наблюдения: Gemini-south

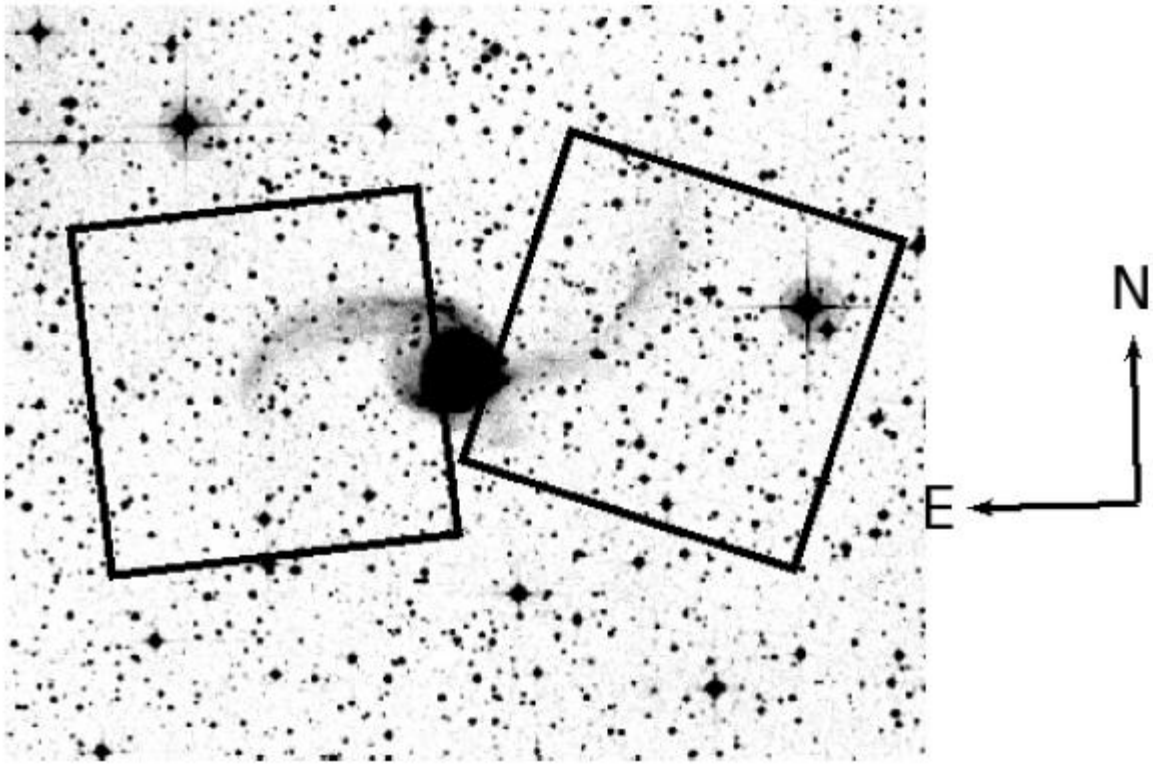

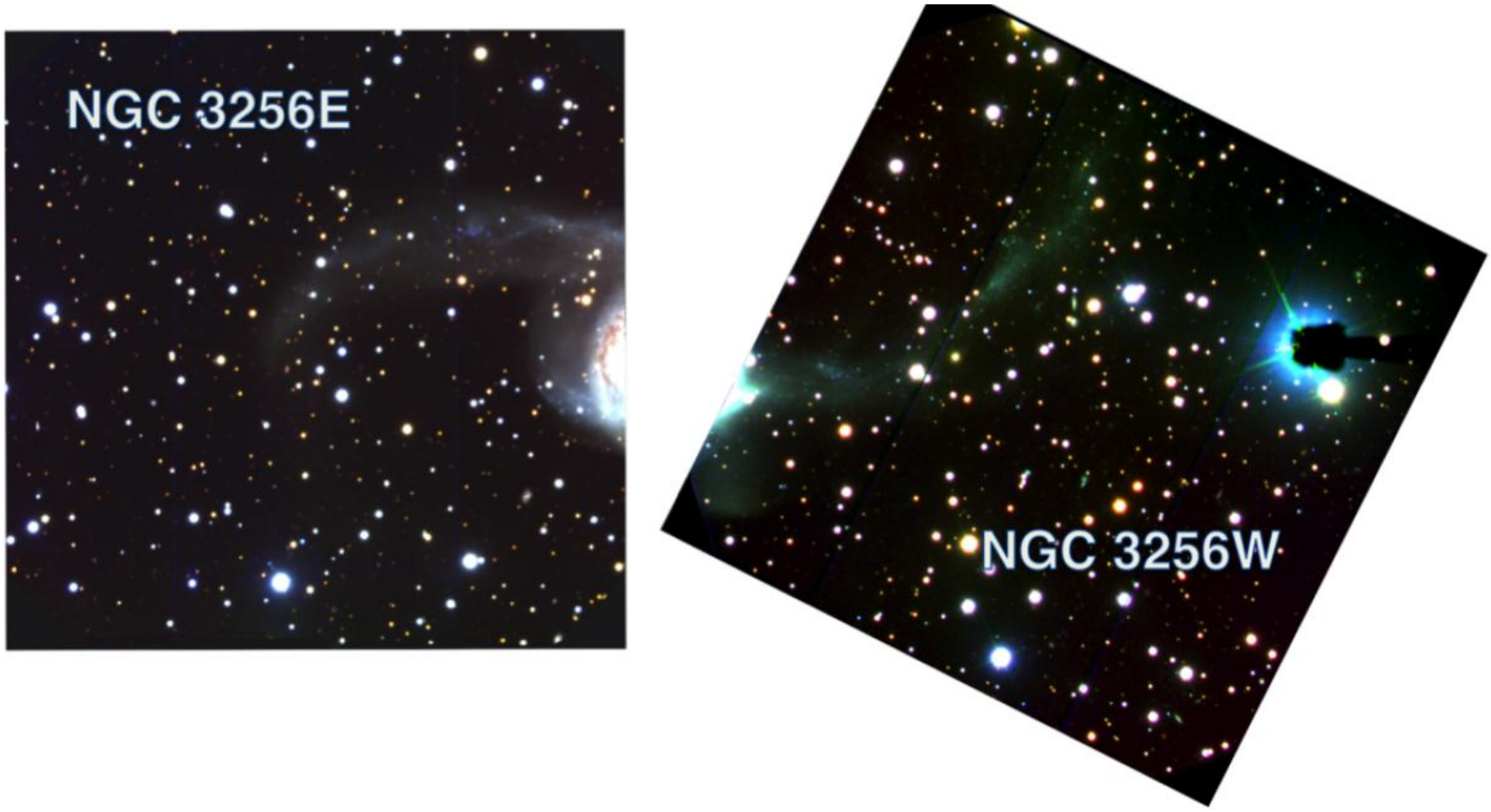

Figure 2. Colour images of NGC 3256E (*left*) and NGC 3256W (*right*) taken with GMOS-S. Combined images in the u-band represent blue, g-band images represent green, and r-band images represent red. In this image, North is up, and East is to the left.

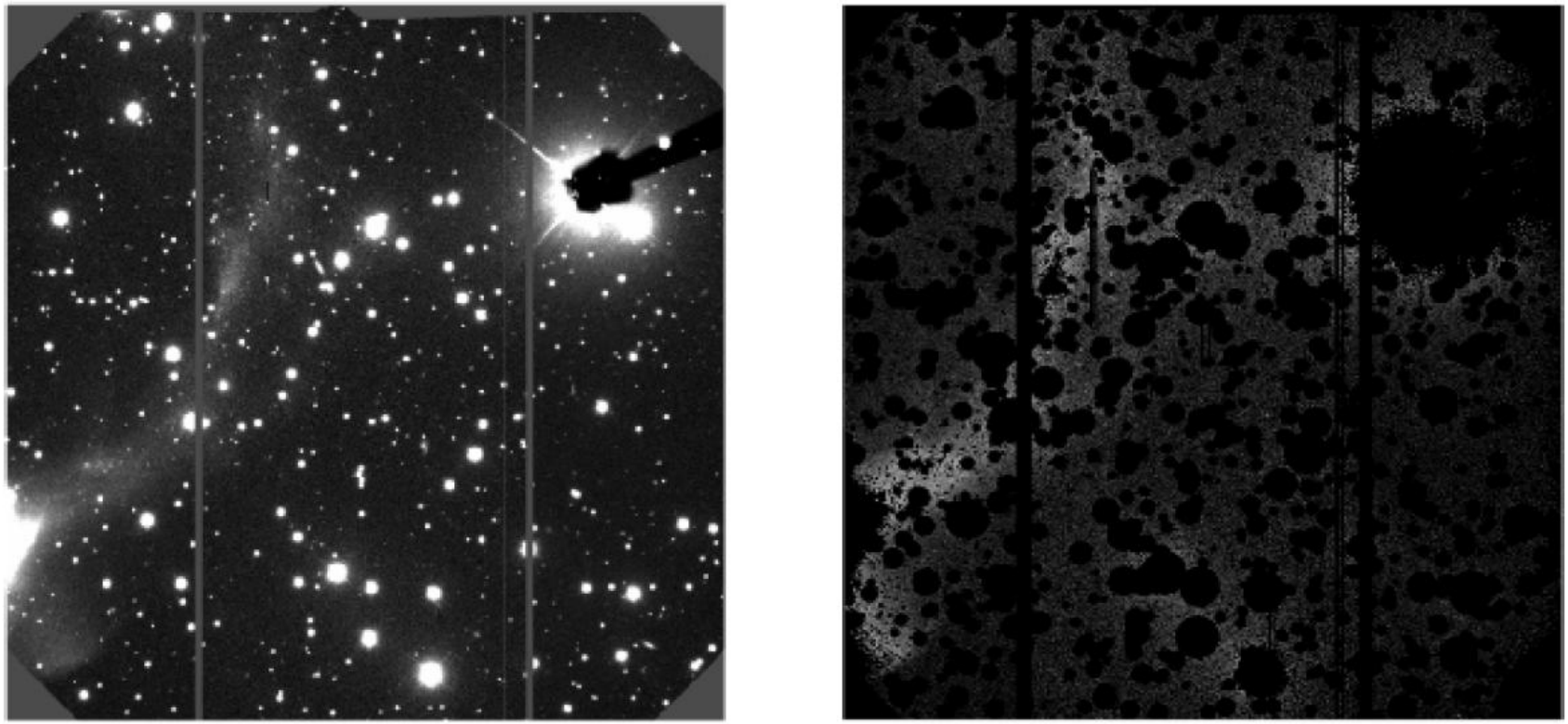

Figure 4. *Left*: g-band image of NGC 3256W. *Right*: Same image, but with the mask applied. The tail light stands out free of contaminant sources. Note the diffuse light from several brighter stars appears in the top and bottom of the image. These objects were saturated and an accurate mask could not be found. However, they are far enough from the tail to not have an effect.

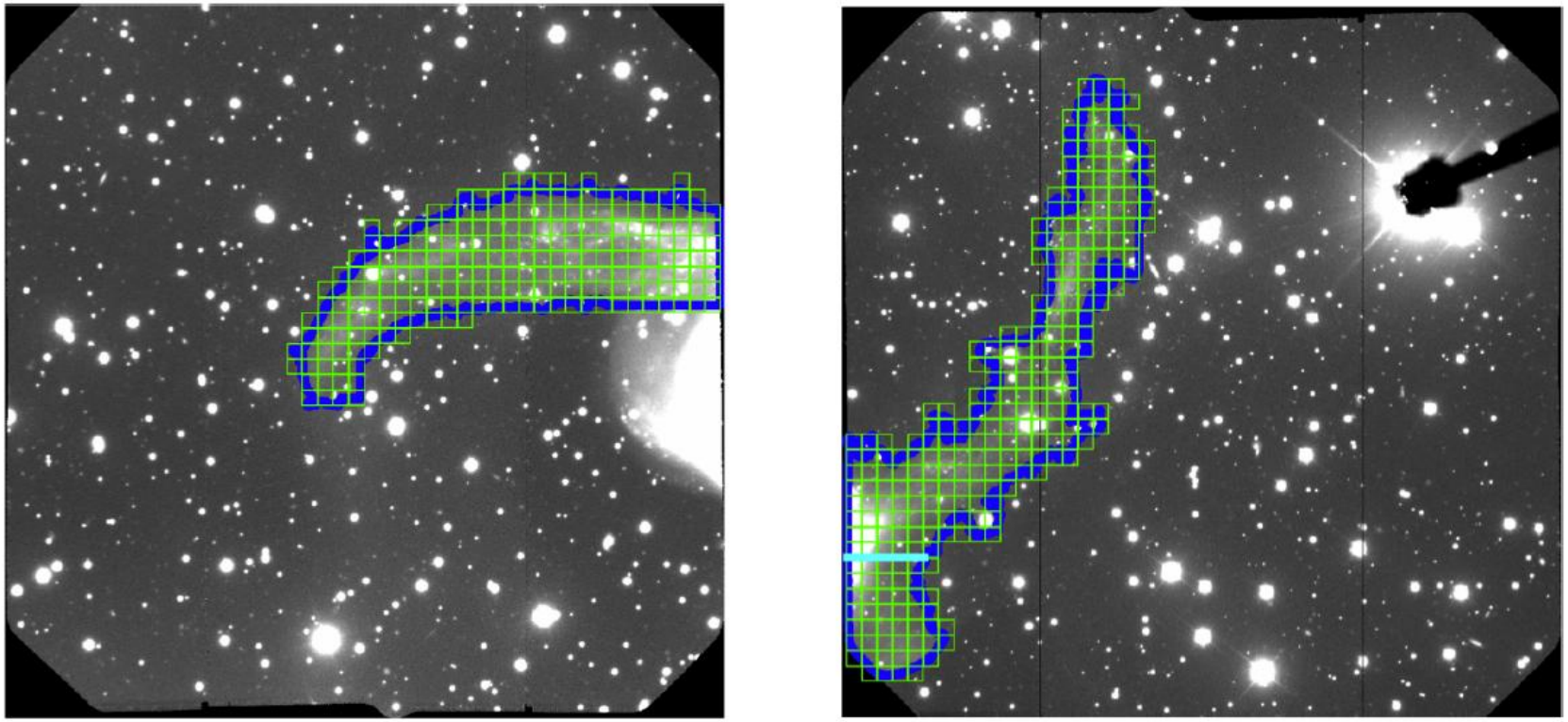

Figure 5. Selected regions for photometry for NGC 3256E (*left*) and NGC 3256W (*right*). Blue lines indicate the boundary of the tail region. In the Western tail, a cyan line indicates the boundary between the tail and diffuse structure. Several boxes are not fully enclosed with the tail, however only pixels within the blue boundary are counted for photometry. We additionally only count boxes with ≥ 50 good pixels.

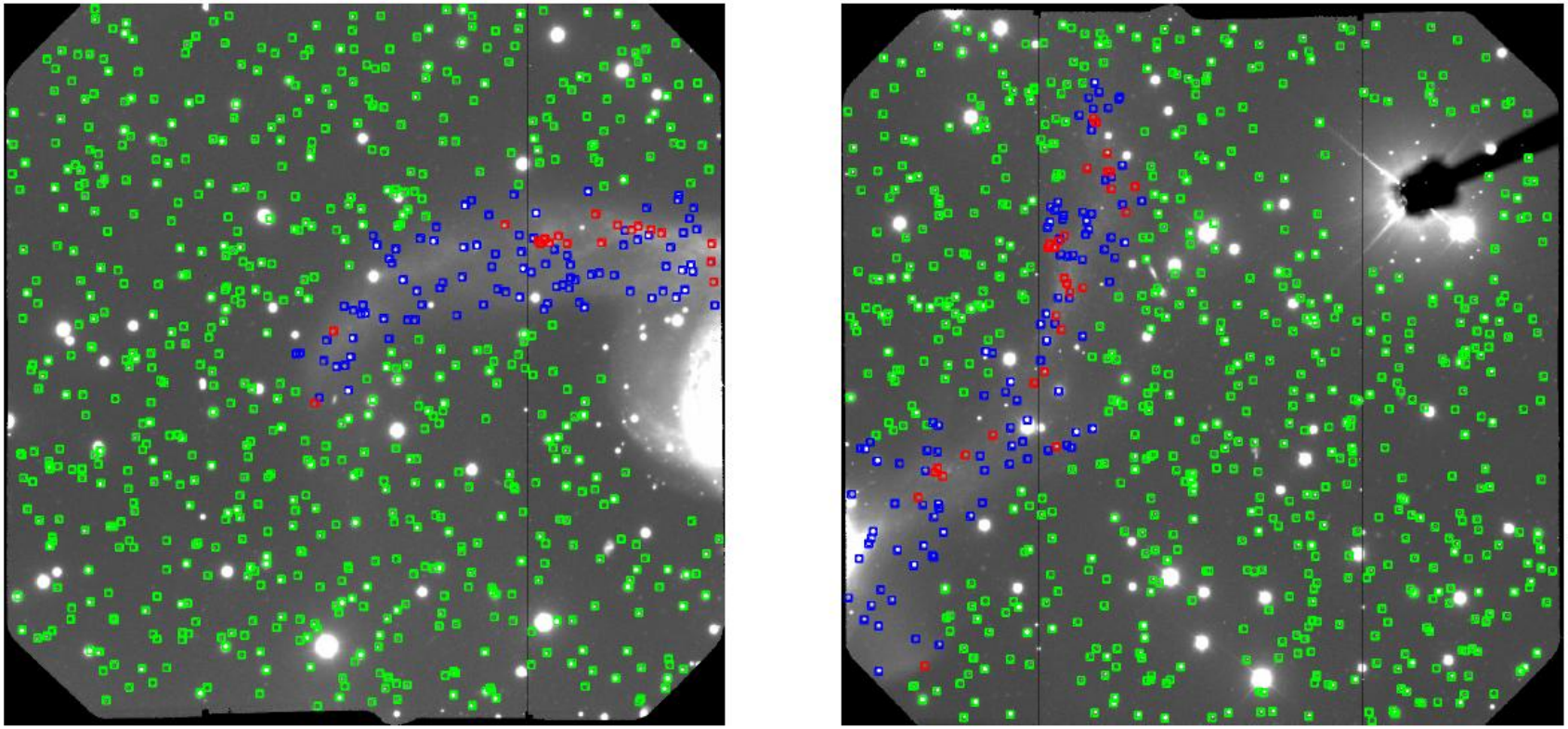

Figure 6. *Left*: Locations for in-tail objects (blue) and out-of-tail objects (green) shown for NGC 3256 E. Red sources are Star Cluster Candidates (SCCs), as determined in Section 4.3.1. *Right*: Same, but for the Western tail.

- Модель: SSP (Marigo+, 2008) и Mixed SSP

(SSP (T)+ 10 Gyr)

Вывод;

Интегральный цвет: 98% массы звезд и 68% болометрической светимости – старые звезды. Вариации вдоль TT.

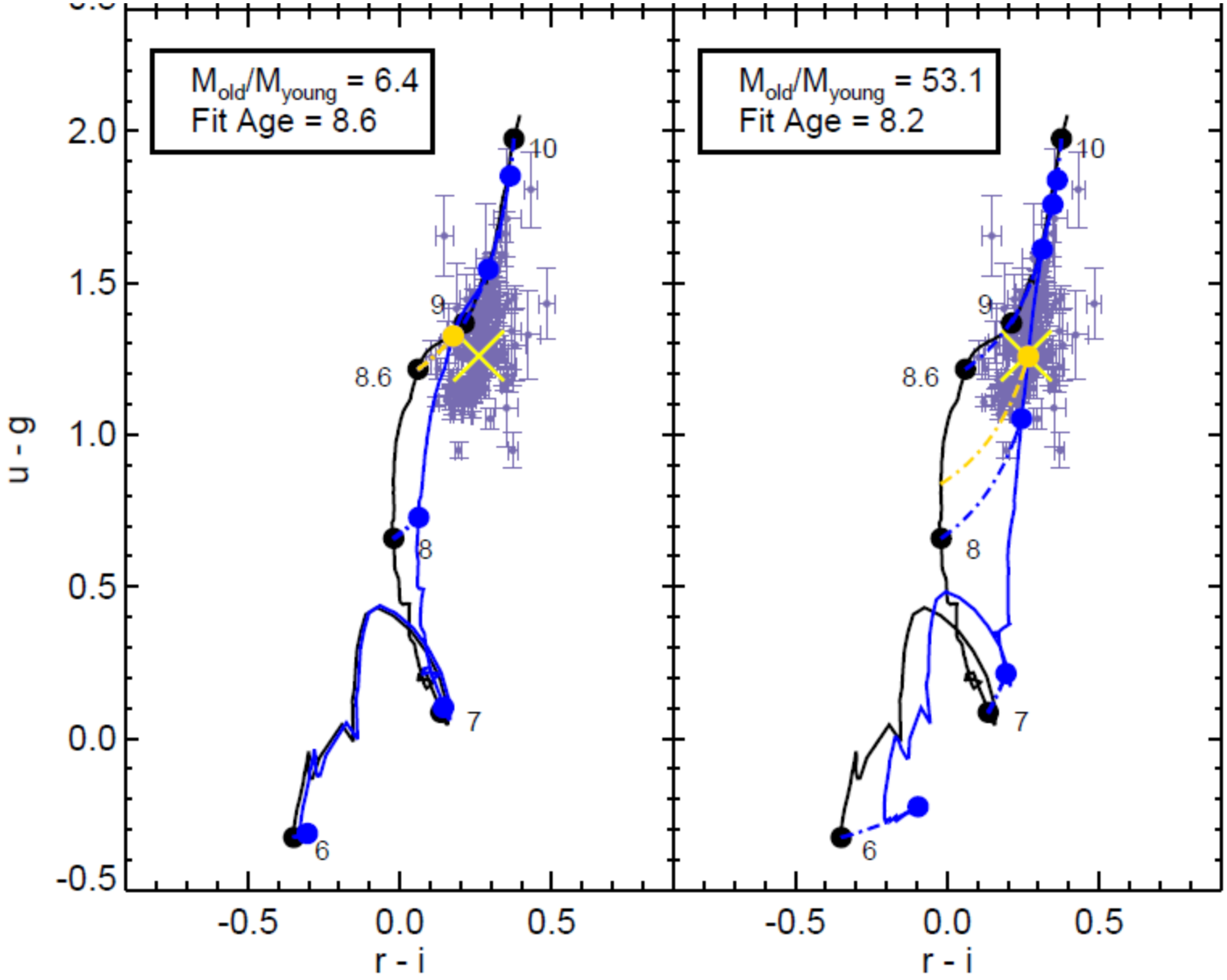
M_{old}/M_{young} = 6.4
Fit Age = 8.6
M_{old}/M_{young} = 53.1
Fit Age = 8.2
u - g
r - i
r - i
10
9
8.6
8
7
6
10
9
8.6
8
7
6
2.0
1.5
1.0
0.5
0.0
-0.5
-0.5
0.0
0.5
-0.5
0.0
0.5

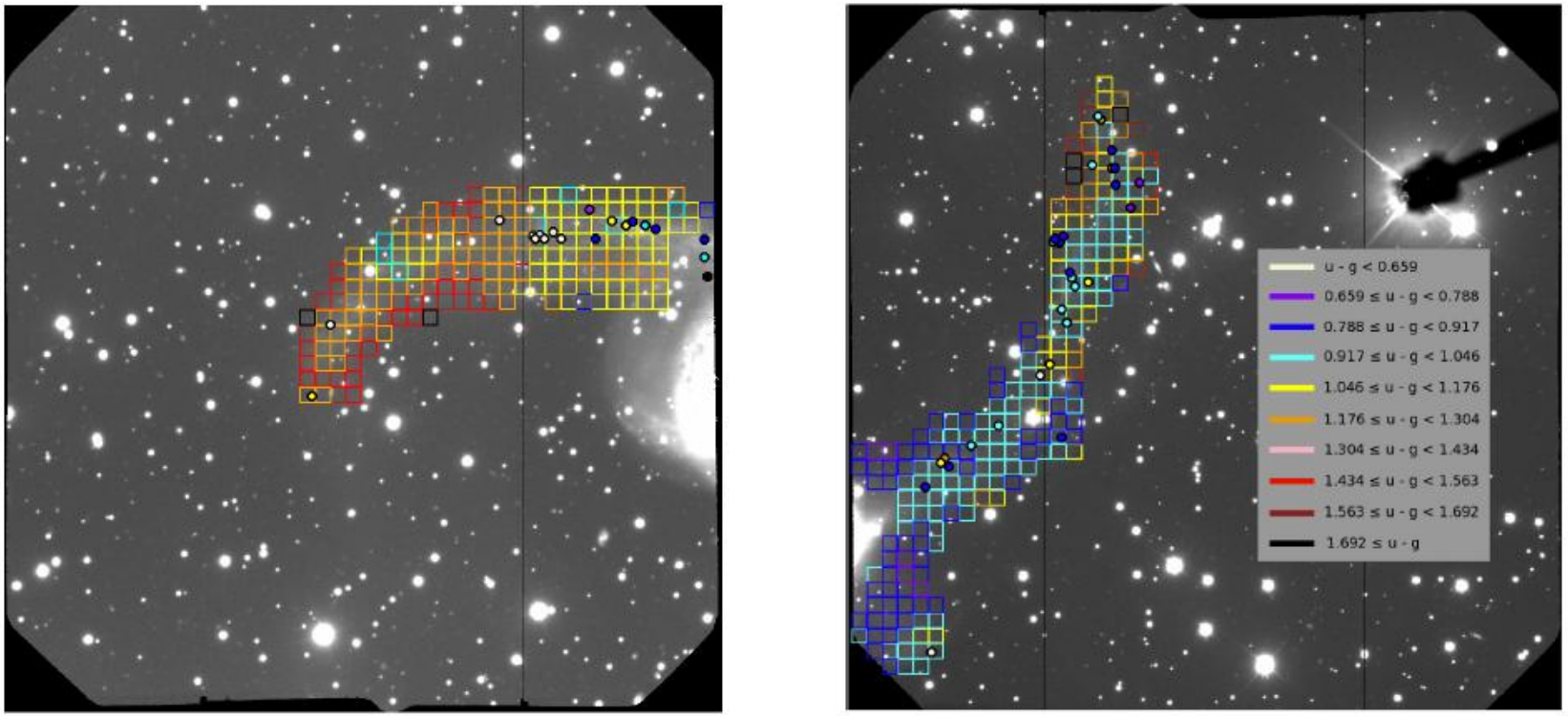

Figure 16. *Left*: Spatial distribution of diffuse light and SCC $u-g$ colours for the Eastern tail. *Right*: Same, but for the Western tail. Colour code is reproduced from Figure 12. Each tail shows a gradient in colour across their length, suggesting a decrease in the fraction of young stars within the diffuse light along the tail from centre to tip.

Tail	Diffuse Old Age (log yrs)	Diffuse Young Age (log yrs)	Median Cluster Age (log yrs)	Diffuse Old Mass ($10^8 M_\odot$)	Diffuse Young Mass ($10^8 M_\odot$)	Star Cluster Mass ($10^8 M_\odot$)	HI Mass[1] ($10^8 M_\odot$)
West	10	$8.29^{-0.03}_{+0.0}$	8.15	$128.3^{+5.6}_{-5.6}$	$15.1^{+0.5}_{-0.5}$	$0.31^{+0.05}_{-0.06}$	22.0
East	10	$8.23^{-0.23}_{+0.11}$	7.96	$392.2^{-2.8}_{+6.1}$	$10.7^{+1.3}_{-1.3}$	$0.13^{+0.04}_{-0.02}$	14.0

Table 4. Mass measurements of NGC 3256, using a Salpeter IMF for stellar mass.
[1]From Knierman et al. (2003)

- Скопления (SCC – Star Cluster Candidates) рождаются преимущественно в областях с низким shear.

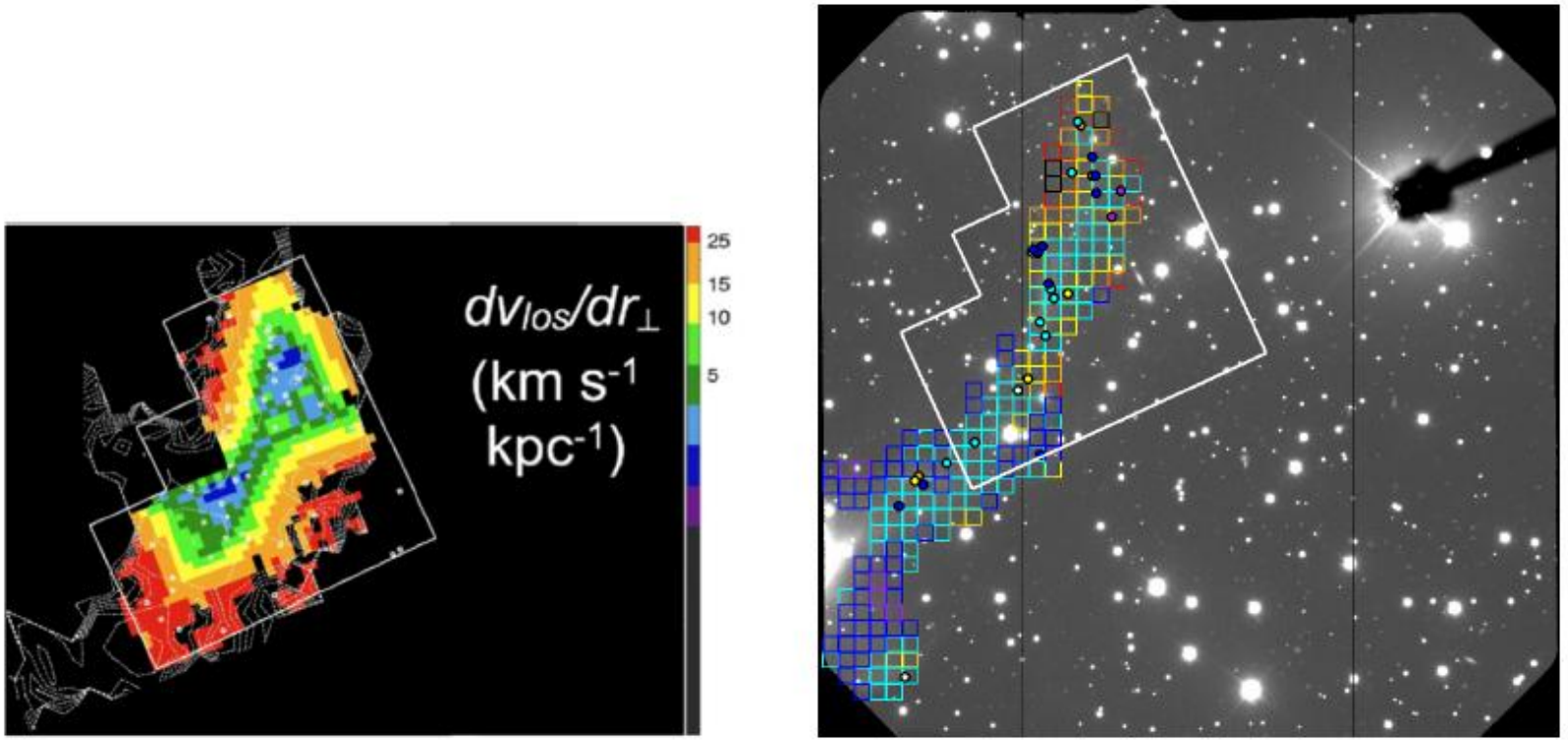

Figure 19. Same as Figure 18, but for the Western tail. The majority of detected SCCs within the WFPC2 footprint lie in the spine of low shear (green and blue in the left-hand panel), with measurements less than 5 km/s/kpc.

Самые главные выводы

- Хвосты содержат преимущественно старые звезды, но различаются по цвету и содержанию молодых звезд: W голубее, чем E, который состоит почти полностью из старых звезд родительской галактики.

В модели MSP возраст молодых звезд в дифф.поле в обоих хвостах – около 200 млн.лет. Возраст скоплений вдвое ниже.

- Среди скоплений нет старше 10^9 лет. В E-хвосте есть несколько скоплений с T<10^7 yr, т.е. SF шло уже в хвосте!
- Молодые скопления рождаются преимущественно в областях с более высокой дисперсией скоростей газа и низким shear. Диффузный свет также голубее в областях с низким shear.